Macromolecules

NOTE

pubs.acs.org/Macromolecules

Controlled Self-Aggregation of C_{60}-Anchored Multiarmed Polyacrylic Acids and Their Cytotoxicity Evaluation

Chih-Chien Chu,*[,†] Ya-Ju Tsai,[†] Li-Chia Hsiao,[†] and Leeyih Wang*[,‡]

[†]School of Applied Chemistry, Chung Shan Medical University, Taichung 40201, Taiwan

[‡]Center for Condensed Matter Science, National Taiwan University, Taipei 10617, Taiwan

Supporting Information

Water-dispersible fullerene (C_{60}) derivatives have been extensively studied for versatile biological applications.[1] More recently, C_{60}-based materials bearing ionic substituents have also been examined as DNA transfection vectors and tested for the ability to mediate gene transfer.[2] Isobe et al. pioneered the potential use of cationic C_{60} derivatives as carriers for gene delivery.[3] They reported a library of 22 aminofullerenes and found that tetra(piperazino)fullerene epoxide showed a 4-fold increase of transfection efficiency compared to lipofectin, a widely used lipid-based transfection agent.[4] This remarkable efficiency is due to a stronger binding between C_{60} and DNA as well as to a suitable complex size around 100 nm in the incubation medium, allowing the C_{60} molecule to shuttle nucleic acids into the cell. It is known that pristine C_{60} is a peculiar solvophobic and water-insoluble molecule.[5] Accordingly, spontaneous self-aggregation of the C_{60} derivatives into large clusters usually takes place in either organic or aqueous solution because of a high affinity of C_{60} moiety toward itself. Therefore, the size control of these aggregates through molecular design is essential for dominating the complexation of C_{60} derivatives and nucleic acids.

A noteworthy drawback of C_{60} derivatives for biomedicinal applications is its cytotoxicity. It has been suggested that one possible reason for such observed cytotoxicity was due to the use of organic solvents such as DMF and DMSO.[3] In other words, polar organic solvents are still required for increasing the overall solubility of those hydrophilic C_{60} adducts toward biological purpose. Moreover, direct modification of multiple hydrophilic moieties onto the C_{60} molecule usually results in a mixture of isomers owing to the multiple reactive sites on the C_{60} surface, and consequently, tedious chromatographic separation of these isomers is inevitable.[6] Within this concern, it is highly expected to synthesize C_{60} derivatives with utmost water solubility and well-defined chemical structure. A family of C_{60}-containing polyelectrolytes is an alternative candidate to fulfill such requirements.[7] First, preparation of water-soluble polyelectrolytes with narrow distribution and specific end-group functionality (e.g., azide, aldehyde) are carried out by controlled polymerization techniques such as atom transfer radical polymerization (ATRP) and reversible addition−fragmentation chain transfer polymerization (RAFT).[8] A facile dipolar addition is then adopted to conjugate the well-defined polyelectrolytes and C_{60} through either a [5,6] or [6,6] junction.[9] Accordingly, thus-prepared C_{60}-containing polymeric architectures not only exhibit high water solubility but also have relatively defined structure because the C_{60}−polymer conjugation due to steric effect exclusively yields a monoadduct.

Scheme 1. Water-Soluble C_{60}-Anchored 2-, 4-, and 8-Armed Polymers (X = COOH)[a]

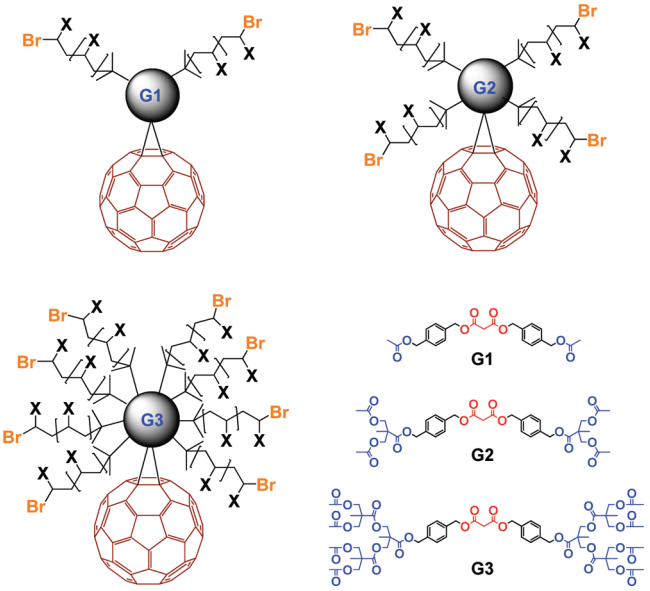

[a] Dendritic G1, G2, and G3 represent the divergent cores for atom transfer radical polymerization.

Furthermore, the primary aggregate of C_{60}-containing polyelectrolytes with nanometer size also satisfies the size requirement for efficient endocytosis.[10]

Our recent effort has demonstrated a novel synthesis route for the preparation of well-defined C_{60}-anchored starburst anionic poly(acrylic acid) (PAA) and found remarkable photoinduced charge transfer between cationic porphyrin and these polymers in aqueous solution.[11] The result clearly suggests that the bulky substituent did not obstruct the charge acceptability of C_{60} toward photoexcited porphyrins that were adsorbed onto the PAA backbone through electrostatic interaction. On the basis of this finding, the present study further examined the self-aggregated behaviors of C_{60}-anchored 2-, 4-, and 8-armed PAA in

Received: June 13, 2011
Revised: July 28, 2011
Published: August 10, 2011

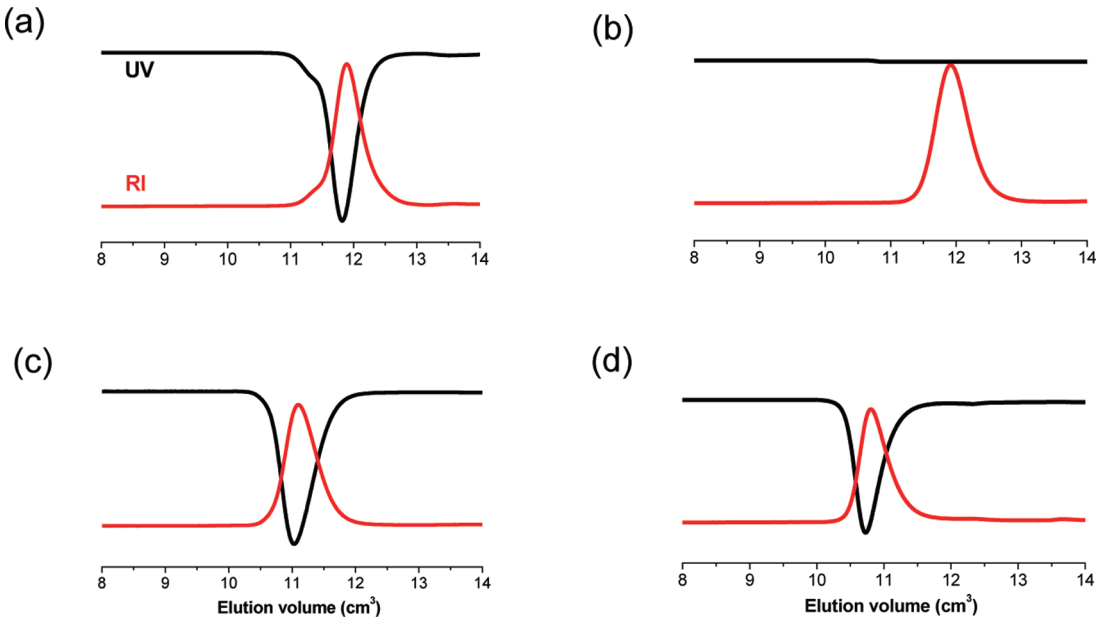

Figure 1. UV (350 nm, black line) and RI (red line) detected GPC traces of (a) C_{60}-anchored 2-armed poly(*tert*-butyl acrylate) (PtBA), (b) 2-armed PtBA prepolymer, (c) C_{60}-anchored 4-armed, and (d) 8-aremd PtBA.

water and evaluated the cytotoxic properties prior to gene or drug delivery using the novel C_{60}-anchored PAA as a carrier.

Scheme 1 depicted the C_{60}-anchored multiarmed polymers via Bingel cyclopropanation of C_{60} with malonate ester-centered star-shaped PtBA, which was divergently prepared using the ATRP method, and then facile deprotection of the pendant *tert*-butyl group under acidic condition yields highly water-soluble C_{60} adducts with multiple PAA arms.[12] The gel permeation chromatography (GPC) analyses using THF as the eluent (Figure 1) reveal single symmetric and narrowly dispersed peaks centered at 11.8, 11.0, and 10.7 cm^3 for C_{60}-anchored 2-, 4-, and 8-armed PtBA, respectively. These refractive index (RI) and UV-dual-detectable traces not only suggest a well-controlled chain growth during ATRP but also indicate a successful cycloaddition of C_{60} molecule and these star-shaped polymers. Furthermore, the use of ATRP elegantly afforded polymer architectures with narrow molecular weight distribution and precisely controlled chain length. Thus we manipulated the degree of polymerization (DP) of each arm for 2-, 4-, and 8-armed PtBA in a close value by carefully controlling the monomer conversion and propagation time to synthesize a series of C_{60}-anchored star-shaped polymers bearing different arm number but identical arm length. As a result, the average DP values for 2-, 4-, and 8-armed PtBA determined by NMR analyses were found to be 58, 64, and 61 per arm, respectively, suggesting the arm length of each star-shaped polymer is almost identical. Moreover, the acidic hydrolysis of pendant *tert*-butyl groups for giving hydrophilic carboxylic acids is insufficient to degrade the acrylate backbone; accordingly, it is assumed that the DP value per arm for C_{60}-anchored multiarmed PtBA and PAA is invariant, and thus the number-averaged molecular weights (M_n) of either C_{60}-anchored PtBA or PAA could be calculated from those DP values. Table 1 summarized the molecular weight characteristics of these star-shaped polymers.

C_{60}-based polymers are known to form self-assembled clusters in polar solvents because of their amphiphilic characteristics. Kawaguchi et al. adopted GPC analyses for determining the ratio

Table 1. Molecular Weight Characteristics of C_{60}-Anchored Multiarmed Polyacrylic Acids (PAA)

C_{60}-anchored PAA	DP/arm[a]	$M_{n,NMR}$[b]	M_w/M_n	$M_{w,GPC\text{-}RI\text{-}MALLS}$[c]	N_{agg}[d]
2-armed	58	9700	1.12	607 800	60
4-armed	64	20300	1.11	575 100	26
8-armed	61	38100	1.10	ND	ND

[a] The number-averaged degree of polymerization (DP) of each arm was determined by ^1H NMR using the peak area ratio of protons on the polymer backbone to the peripheral methyl protons on the divergent cores. [b] The number-averaged molecular weights were calculated from DP of each arm using the formula: $M_n = (DP \times M \times n) + M_i + 720$, where M, M_i, and 720 stand for the molar mass of the repeating AA unit, core, and C_{60}, respectively; n stands for the arm number. [c] The weight-averaged molecular weights (M_w) were determined by the GPC method using online refractive index (RI) and multiple angle laser light scattering (MALLS) dual detectors. [d] The aggregation number (N_{agg}) was calculated from the quotient of the aggregated M_w and the unimeric M_w determined by GPC-RI-MALLS and NMR, respectively, on the basis of a quite narrow polydispersity (M_w/M_n = 1.1).

of aggregated and nonaggregated C_{60}-end-capped poly(methyl methacrylate) in H_2O/CH_3CN mixture.[13] In our study, the self-assembly behaviors of water-soluble C_{60}-anchored 2-, 4-, and 8-armed PAA, composed of hydrophilic PAA arms and hydrophobic C_{60} core, were also examined by GPC method using aqueous solution as the mobile phase straightforwardly. Figure 2 shows the RI-detected traces of the C_{60}-anchored polymer solutions after the samples had been dialyzed for 24 h against water and then dried by lyophilization. The chromatogram of C_{60}-anchored 2-armed PAA (Figure 2a) clearly exhibits two distinct peaks centered at 6.4 and 7.8 cm^3, where the latter is quite close to the peak of 2-armed PAA prepolymer lacking of C_{60} anchoring at 8.0 cm^3 (Figure 2b). Because the molar mass of C_{60}-anchored PAA was almost identical with that of its PAA precursor, it is reasonable to hypothesize that the elution peaks

dx.doi.org/10.1021/ma2013404 |*Macromolecules* 2011, 44, 7056–7061

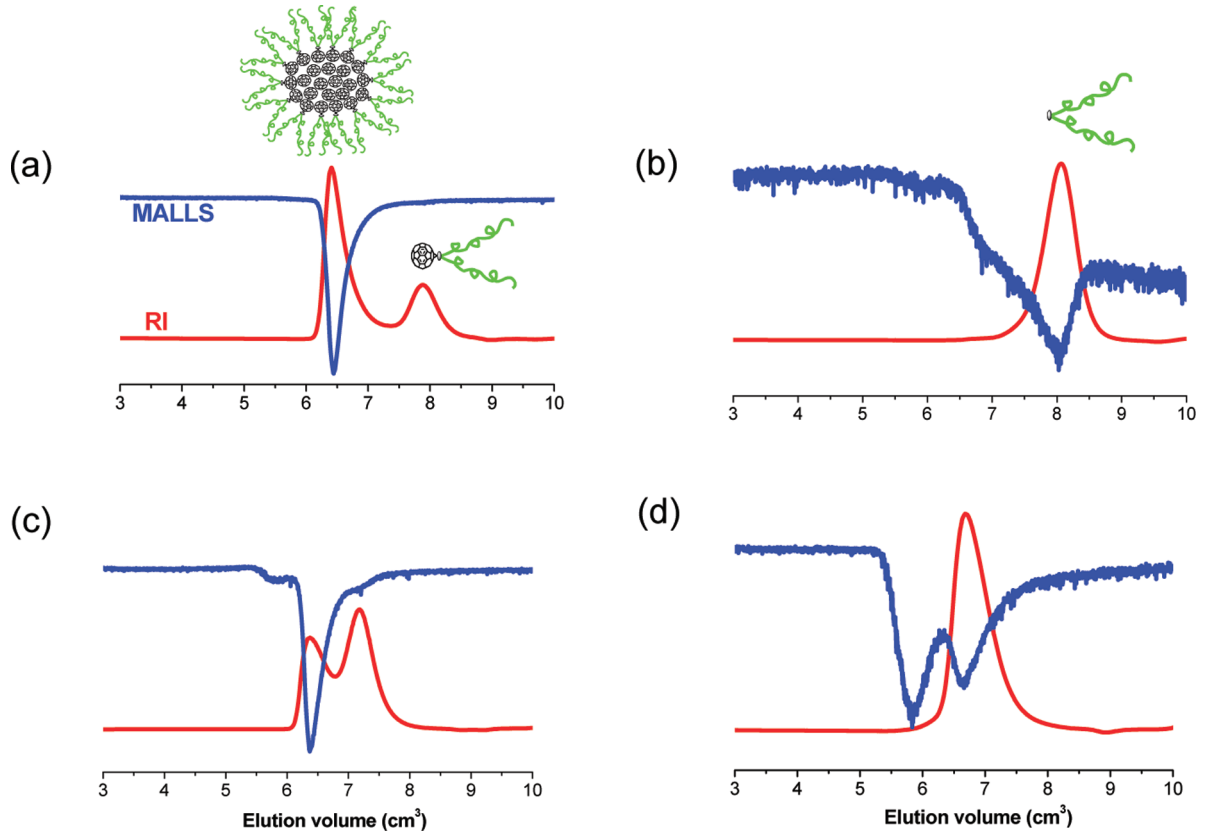

Figure 2. RI (red line) and MALLS (blue line) detected GPC traces of (a) C_{60}-anchored 2-armed poly(acrylic acid) (PAA), (b) 2-armed PAA prepolymer, (c) C_{60}-anchored 4-armed, and (d) 8-aremd PAA.

centered at 7.8 and 8.0 cm^3 in Figure 2a,b, respectively, stand for two individual polymers bearing similar molecular weights and that the peak at lower elution volume (6.4 cm^3) corresponds to the self-aggregated clusters with higher molecular weights.[14] Although the facile GPC-RI analysis clearly indicates the coexistence of self-aggregation and individual chains, the reliable molar mass for these components cannot be determined by a conventional calibration method established by linear polymer standards because of a globular nature of these clusters and star-shaped polymers. In addition, on the basis of a simple integration of the peak areas, 76% of C_{60}-anchored 2-armed PAA was involved in the aggregation process. In contrast, the self-aggregation of 2-armed PAA prepolymer was completely absent in the GPC analysis under identical conditions, suggesting that C_{60} moiety did induce the micelle-like aggregation of the amphiphilic C_{60}-anchored 2-armed polymer into large clusters with C_{60} core and PAA shell.

The self-aggregation of C_{60}-anchored 4- and 8-armed PAA in water was also monitored by GPC-RI analysis. Figure 2c displayed two peaks centered at 6.3 and 7.1 cm^3 corresponding to the aggregated cluster and unimer of C_{60}-anchored 4-armed stars, respectively, whereas only the individual C_{60}-anchored 8-armed star was observed as a single symmetric peak at 6.7 cm^3 (Figure 2d). This remarkable diminishing of the C_{60}-induced aggregation was mainly attributed to the higher hydrophilic—lipophilic balance (HLB) between C_{60} and 8-armed PAA.[15] First of all, the fullerene content for the C_{60}-anchored multiarmed polymers drops as the arm number grows geometrically. Therefore, the hydrophilic 8-armed PAA is capable of subduing the intermolecular association of C_{60} cores, where the 8-armed system has the lowest fullerene content (1.1%). Furthermore, the 8-armed PAA provides an umbrella-like shielding toward the solvophobic C_{60} core to achieve a better HLB, and therefore the aggregation of C_{60}-anchored 8-armed PAA was absent in water. In the cases of 2- and 4-armed systems, higher fullerene contents and relatively poor HLB between PAA and C_{60} results in the formation of micelle-like aggregates. Interestingly, the ratio of the aggregated C_{60}-anchored 4-armed stars was found to be 41%, but 76% of the 2-armed stars aggregated in water. In other words, the self-aggregated clusters predominate in the 2-armed system, but C_{60}-anchored 4-armed PAA favors the presence in unimeric structure. The HLB of PAA building blocks and C_{60} core apparently account for the difference in aggregation level and, notably, the fraction of aggregated C_{60}-anchored multiarmed PAA drastically decreases as the arm number propagates.

The GPC method only provides the relative molecular weights and often underestimates the M_n values of branched polymers, e.g., dendrimers and star-shaped polymers, because they have a more globular architecture than linear polymers, causing the molecules to be smaller than random-coiled standards.[16] Therefore, we adopted the online GPC-RI-multiple angle laser light scattering (MALLS) detection for determining the absolute molar mass of the aggregated clusters with a star-shaped nature. According to the model proposed by Wyatt and co-workers,[17] the conventional Zimm plot relationship under GPC condition can be expressed as eq 1 on the basis of the assumption that the second viral coefficient (A_2) and analyte

dx.doi.org/10.1021/ma2013404 |*Macromolecules* 2011, 44, 7056–7061

concentration (c) approach zero in a dilute system:

$$\frac{R_\theta}{Kc} = \frac{M_w}{\left[1 + 16\pi^2 n^2 \langle R_g^2 \rangle \sin^2\left(\frac{\theta}{2}\right)/3\lambda^2\right]} \quad (1)$$

where R_θ is the excess Rayleigh ratio at the scattering angle θ; $K = 4\pi n^2 (dn/dc)^2 \lambda_0^{-4} N_A^{-1}$ is an optical constant; n is the refractive index of the mobile phase; (dn/dc) is the refractive index increment of the polymer solution; λ_0 is the wavelength of laser light; N_A is Avogadro's constant. A Debye plot of R_θ/Kc versus $\sin^2(\theta/2)$ can be fitted by the polynomial method and thereby obtain the intercept as the weight-averaged molecular weights (M_w) at zero angle.

The GPC-MALLS chromatograms of C_{60}-anchored 2- and 4-armed PAA (Figure 2a,c) only show an intensive peak at 6.4 and 6.3 cm^3, respectively, which occupies the same elution volume of the aggregated clusters detected by RI, whereas the 2-armed PAA prepolymer dissolving in water individually only reveals a much weaker and less resolved signal at 8.0 cm^3 (Figure 2b). This result clearly confirms that the RI and MALLS-dual-detectable trace in Figure 2a,c is attributed to the C_{60}-induced self-aggregated clusters with higher molar mass and larger dimension in which the scattering intensity is stronger, and that the MALLS signal of individual polymers was completely excluded because of the lower molar mass as well as the small size. However, the C_{60}-anchored 8-armed PAA exhibits a different elution pattern that both aggregates (5.8 cm^3) and unimers (6.7 cm^3) can be detected as less intense peaks by MALLS detection, whereas the RI only notices the latter. It is known that the light scattering detection method is highly sensitive to the giant macromolecular architectures. Therefore, the result suggests that the C_{60}-anchored 8-armed PAA partially forms the self-aggregated clusters whose concentration is lower than the detection limit of the RI detector, but the MALLS detection is capable of sensing the presence of the micelle-like structures in a dilute condition.

On the basis of eq 1, where the concentration (C) can be obtained from RI analysis, we further estimate the M_w values for the aggregated C_{60}-anchored 2- and 4-armed PAA by constructing the Debye plot under eight scattering angles. Table 1 lists the molecular weight characteristics and calculated aggregation number (N_{agg}) of C_{60}-anchored polymers. Interestingly, the self-aggregated clusters of C_{60}-anchored 2- and 4-armed PAA have quite close M_w values, although these two systems have different fullerene contents and arm numbers, and thus the N_{agg} determined for 4-armed polymer (~26) is approximately half of that for 2-armed polymer (~60). It is assumed that a higher HLB between C_{60} core and 4-armed PAA, holding a 2-fold increase in the amount of the acrylic acid (AA) units, accounts for the lower N_{agg} values. Notably, the N_{agg} values of the C_{60}-anchored multi-armed polymers are much lower than that of the mono and dual fullerene-end-capped polymers with similar molecular weights,[15b] implying the lipophilicity of the C_{60} moiety is more effectively subdued by the divergent hydrophilic arms as we functionalized the C_{60} molecule at the focal point instead of the chain ends. In addition, Figure 3 demonstrates that either the N_{agg} values or the fraction of nonaggregated polymers (F_{nonagg}) is proportional to the naturally logarithmic PAA arm numbers, which not only indicated that the C_{60}-induced aggregation is well-controlled by the number of pendant PAA arms but also implied that the aggregation process through HLB of the amphiphiles (PAA arms and C_{60} core) behaves thermodynamically.

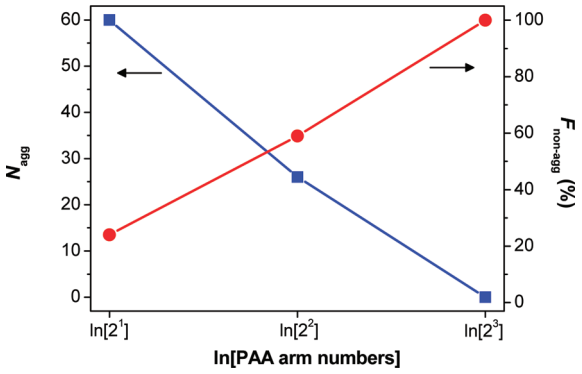

Figure 3. Correlation between the aggregation number (N_{agg}) and the fraction of nonaggregated polymers (F_{nonagg}) with naturally logarithmic PAA arm numbers. The N_{agg} values were estimated from the MALLS and RI detected GPC peaks of the aggregated clusters; F_{nonagg} was determined on the basis of the RI detected GPC peak areas of the unimers.

The dimension of aggregated C_{60}-anchored polymers was examined by different methods carried out in both solution and solid states. Dynamic light scattering measurement for C_{60}-anchored 2-armed PAA shows a z-average dimension around 13 nm with a polydispersity index of 0.27 (Figure 4a), which is also much smaller than the aggregated size of the C_{60}-end-capped polymers in water.[15d] Atomic force microscopy (AFM) and electron transmittance microscopy (TEM) were performed to confirm the morphology of aggregated C_{60}-anchored 2-armed PAA; the AFM micrograph (Figure 4b) displays isolated nanoparticles with diameter distribution from 20 to 40 nm, and TEM image (Figure 4c) also reveals nearly spherical aggregates with a mean diameter of 35 nm. Furthermore, the ζ potential measurement revealed that the surface of these aggregated clusters was negatively charged (−44.8 mV), suggesting the polyanionic PAA peripherals indeed stabilize the aggregated C_{60} core. Although there was a noticeable discrepancy in particle dimension estimated from solution and solid state, the result taking all into account concludes the formation of the core−shell-like micelles composed of the amphiphilic C_{60}-anchored PAA through primary aggregation.

The cytotoxicity of carbon-based nanomaterials such as C_{60} and carbon nanotubes (CNT) aroused much attention prior to their biomedicinal applications.[18] However, poor solubility of either pristine C_{60} or its derivatives in aqueous environment usually restricts the convinced and reproducible toxicity study in vitro and in vivo. In our case, the highly water-soluble C_{60}-anchored 2-armed PAA allows the concentration-dependent cytotoxicity of C_{60} to be straightforwardly estimated using MTT assay in aqueous buffer medium.[19] Though the previous research proposed that the toxicity of C_{60} derivatives was nonspecific to cell types, the cell viability test was accessed in vitro toward rat C6 glioma cells and human MCF-7 cells for comparison.[20] As shown in Figure 5, for C6 cell lines, the 2-armed PAA prepolymer was slightly toxic up to a dose of 200 $\mu g/cm^3$ (89 ± 3.3% cell viability), and the C_{60}-anchored PAA was more toxic (70 ± 1.6% cell viability); for MCF-7 cell lines, the cytotoxicity of C_{60}-anchored PAA (79 ± 2.5% cell viability) was also higher than that of the prepolymer (88 ± 3.1% cell viability). As expected, the result not only presented a dose-dependent effect on cellular toxicity toward two cell lines but also suggested that different expression of C_{60}-anchored PAA and its prepolymer is largely

dx.doi.org/10.1021/ma2013404 |*Macromolecules* 2011, 44, 7056–7061

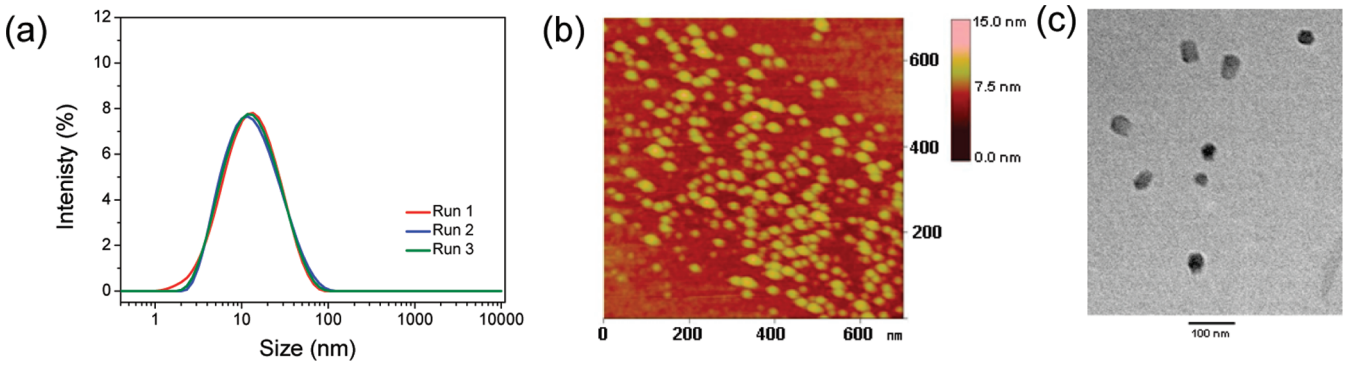

Figure 4. Size distribution analyses of C_{60}-anchored 2-armed PAA obtained from (a) dynamic light scattering (DLS), (b) atomic force microscopy (AFM), and (c) transmittance electron microscopy (TEM).

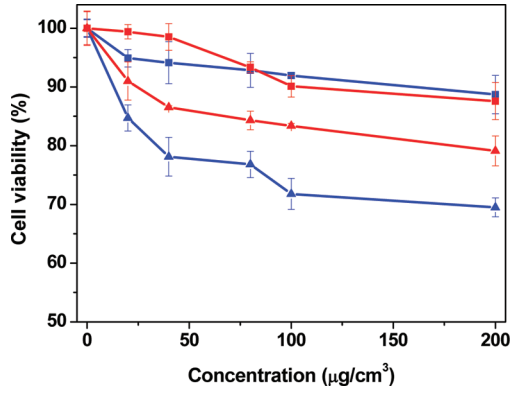

Figure 5. In vitro cytotoxicity of C_{60}-anchored 2-armed PAA toward rat C6 glioma cells (blue line) and human MCF-7 cells (red line) at various concentrations. Cellular viability was evaluated by MTT assay. Data are the mean of four experiments in triplicate ± SD.

due to the intrinsic toxicity of fullerene core. Although our study clearly indicates that the C_{60} moiety might enhance the overall toxicity of the fullerene-functionalized nanomaterials, the nanoclusters of C_{60}-anchored 2-armed PAA are still highly expected as carriers for compatible drugs and genes because of their micelle-like structure as well as their moderate cytotoxicity.

In summary, we adopted the GPC method using online RI and MALLS dual detections instead of the batch mode LLS system to analyze the self-aggregated behavior of C_{60}-anchored multi-armed PAA in aqueous solution. The result indicated that C_{60}-anchored 2-armed PAA favors the formation of self-aggregated clusters with a C_{60} core and PAA shell, whereas the aggregation of 8-armed polymers is almost absent in water. The different behaviors for these C_{60}-anchored polymers are attributed to the different HLB between C_{60} core and divergent arms, which is the 8-armed PAA is capable of subduing the intermolecular association of C_{60} completely. Moreover, DLS, AFM, and TEM all confirmed a nanometer dimension with nearly spherical shape for aggregated clusters of 2-armed polymer, and ζ potential measurements also revealed the multiple negative charges generated from the AA units on particle surface. Although the MTT assay suggested that the C_{60}-anchored 2-armed PAA has certain in vitro cytotoxicity when compared with its 2-armed prepolymer, the nanoclusters composed of C_{60}-anchored multiarmed PAA are still promising candidates as carriers for compatible drugs and genes toward clinical therapy. It is also speculated that strong affinity of the C_{60} toward itself is capable of associating the core moiety firmly and thus increases the overall stability of the core−shell-like structures against the biological environment. Furthermore, the fullerene-based micelles not only serve as the carrier but also potentially provide additional functions such as the scavenging for reactive oxygen species and contrast agents for diagnostic imaging.[21] A preliminary study along this line is now underway and will be reported in due course.

■ ASSOCIATED CONTENT

Supporting Information. Experimental details regarding sample preparation, GPC analyses, and in vitro cytotoxicity assay. This material is available free of charge via the Internet at http://pubs.acs.org.

■ AUTHOR INFORMATION

Corresponding Author

*C.-C.C.: fax, +886-4-2324-8189; e-mail, jrchu@csmu.edu.tw. L.W.: tel, +886-2-3366-5276; e-mail, leewang@ntu.edu.tw

■ ACKNOWLEDGMENT

C.-C.C. thanks Chung Shan Medical University and the National Science Council of Taiwan, Republic of China, for financially supporting this research (NSC98-2113-M-040-003-MY2).

■ REFERENCES

(1) Nakamura, E.; Isobe, H. *Acc. Chem. Res.* **2003**, *36*, 807–815.

(2) (a) Sitharaman, B.; Zakharian, T. Y.; Saraf, A.; Misra, P.; Ashcroft, J.; Pan, S.; Pham, Q. P.; Mikos, A. G.; Wilson, L. J.; Engler, D. A. *Mol. Pharm.* **2008**, *5*, 567–578. (b) Klumpp, C.; Lacerda, L.; Chaloin, O.; Ros, T. D.; Kostarelos, K.; Prato, M.; Bianco, A. *Chem. Commun.* **2007**, 3762–3764.

(3) Isobe, H.; Nakanishi, W.; Tomita, N.; Jinno, S.; Okayama, H.; Nakamura, E. *Mol. Pharm.* **2006**, *3*, 124–134.

(4) (a) Maeda-Mamiya, R.; Noiri, E.; Isobe, H.; Nakanishi, W.; Okayama, K.; Doi, K.; Sugaya, T.; Izumi, T.; Homma, T.; Nakamura, E. *Proc. Natl. Acad. Sci. U. S. A.* **2010**, *107*, 5339–5344. (b) Isobe, H.; Nakanishi, W.; Tomita, N.; Jinno, S.; Okayama, H.; Nakamura, E. *Chem. Asian J.* **2006**, *1*−*2*, 167–175.

(5) Deguchi, S.; Alargova, R. G.; Tsuji, K. *Langmuir* **2001**, *17*, 6013–6017.

(6) Hirsch, A.; Brettreich, M. *Fullerenes: chemistry and reactions*; Wiley-VCH: Weinheim, 2005; pp 289−344.

(7) (a) Giacalone, F.; Martin, N. *Adv. Mater.* **2010**, *22*, 4220–4248. (b) Dai, S.; Ravi, P.; Tam, K. C. *Soft Matter* **2008**, *4*, 435–449.

(8) (a) Inglis, A. J.; Pierrat, P.; Muller, T.; Brase, S.; Barner-Kowollik, C. *Soft Matter* **2010**, *6*, 82–84. (b) Li, C.; Hu, J.; Yin, J.; Liu, S. *Macromolecules* **2009**, *42*, 5007–5016. (c) Hong, S. W.; Kim, D. Y.; Lee, J. U.; Jo, W. H. *Macromolecules* **2009**, *42*, 2756–2761.
(9) Taylor, R.; Walton, D. R. M. *Nature* **1993**, *363*, 685–693.
(10) Gary, D. J.; Puri, N.; Won, Y. Y. *J. Controlled Release* **2007**, *121*, 64–73.
(11) Chu, C. C.; Ho, T. I.; Wang, L. *Macromol. Rapid Commun.* **2007**, *28*, 200–204.
(12) Chu, C. C.; Ho, T. I.; Wang, L. *Macromolecules* **2006**, *39*, 5657–5668.
(13) Kawauchi, T.; Kumaki, J.; Yashima, E. *J. Am. Chem. Soc.* **2006**, *128*, 10560–10567.
(14) Astafieva, I.; Zhong, X. F.; Eisenberg, A. *Macromolecules* **1993**, *26*, 7339–7352.
(15) (a) Yu, H.; Gan, L. H.; Hu, X.; Gan, Y. Y. *Polymer* **2007**, *48*, 2312–2321. (b) Ravi, P.; Wang, C.; Dai, S.; Tam, K. C. *Langmuir* **2006**, *22*, 7167–7174. (c) Ravi, P.; Dai, S.; Tam, K. C. *J. Phys. Chem. B* **2005**, *109*, 22791–22798. (d) Ravi, P.; Dai, S.; Tan, C. H.; Tam, K. C. *Macromolecules* **2005**, *38*, 933. (e) Yang, J.; Li, L.; Wang, C. *Macromolecules* **2003**, *36*, 6060–6065.
(16) (a) Heise, A.; Nguyen, C.; Malek, R.; Hedrick, J. L.; Frank, C. W.; Miller, R. D. *Macromolecules* **2000**, *33*, 2346–2354. (b) Ueda, J.; Kamigaito, M.; Sawamoto, M. *Mscromolecules* **1998**, *31*, 6762–6768.
(17) Wyatt, P. J. *Anal. Chim. Acta* **1993**, *272*, 1–40.
(18) (a) Park, E.-J.; Kim, H.; Kim, Y.; Yi, J.; Choi, K.; Park, K. *Toxicol. Appl. Pharmacol.* **2010**, *244*, 226–233. (b) Kang, S.; Mauter, M. S.; Elimelech, M. *Environ. Sci. Technol.* **2009**, *43*, 2648–2653. (c) Stoilova, O.; Jérôme, C.; Detrembleur, C.; Mouithys-Mickalad, A.; Manolova, N.; Rashkov, I.; Jérôme, R. *Polymer* **2007**, *48*, 1835–1843.
(19) Mosmann, T. *J. Immunol. Methods* **1983**, *65*, 55–63.
(20) Isakovic, A.; Markovic, Z.; Todorovic-Markovic, B.; Nikolic, N.; Vranjes-Djuric, S.; Mirkovic, M.; Dramicanin, M.; Harhaji, L.; Raicevic, N.; Nikolic, Z.; Trajkovic, V. *Toxicol. Sci.* **2006**, *91*, 173–183.
(21) (a) Yin, J. J.; Lao, F.; Fu, P. P.; Wamer, W. G.; Zhao, Y.; Wang, P. C.; Qiu, Y.; Sun, B.; Xing, G.; Dong, J.; Liang, X. J.; Chen, C. *Biomaterials* **2009**, *30*, 611–621. (b) Kato, S.; Aoshima, H.; Saitoh, Y.; Miwa, N. *Bioorg. Med. Chem. Lett.* **2009**, *19*, 5293–5296. (c) Zhang, E. Y.; Shu, C. Y.; Feng, L.; Wang, C. R. *J. Phys. Chem. B* **2007**, *111*, 14223–14226. (d) Shu, C. Y.; Gan, L. H.; Wang, C. R.; Pei, X. L.; Han, H. B. *Carbon* **2006**, *44*, 496–500.